

Infrared Spectrum and Structure of the Hf(OH)<sub>4</sub> Molecule

Xuefeng Wang and Lester Andrews\*

Department of Chemistry, University of Virginia, McCormick Road, P.O. Box 400319, Charlottesville, Virginia 22904-4319

Received April 21, 2005

Laser-ablated Hf atoms react with H<sub>2</sub>O<sub>2</sub> and with H<sub>2</sub> + O<sub>2</sub> mixtures in solid argon to form the Hf(OH)<sub>2</sub> and Hf(OH)<sub>4</sub> molecules, which are identified from the effect of isotopic substitution on the matrix infrared spectra. Electronic structure calculations at the MP2 level varying all bond lengths and angles converge to nearly linear and tetrahedral molecules, respectively, and predict frequencies for these new product molecules and mixed isotopic substituted molecules of lower symmetry that are in excellent agreement with observed values, which confirms the identification of these hafnium hydroxide molecules. This work provides the first evidence for a metal tetrahydroxide molecule and shows that the metal atom reaction with H<sub>2</sub>O<sub>2</sub> in excess argon can be used to form pure metal tetrahydroxide molecules, which are not stable in the solid state.

## Introduction

Metal hydroxide chemistry is dominated by the ionic alkali (NaOH) and alkaline earth metal (Ba(OH)<sub>2</sub>) compounds, which are strongly basic in aqueous solutions. A number of trihydroxides are known, notably those of Al, Sc, Cr, Fe, Co, and the rare earth metals, but there is apparently no evidence for a metal tetrahydroxide compound.<sup>1–4</sup> Furthermore, there are no reports of pure early transition metal hydroxides although some Zr and Hf hydroxy salt complexes such as the sulfates and their hydrates Zr(OH)<sub>2</sub>SO<sub>4</sub> and Hf(OH)<sub>2</sub>SO<sub>4</sub>(H<sub>2</sub>O) have been characterized.<sup>2</sup> Gas-phase investigation is limited to the simple monohydroxide molecules such as LiOH, CaOH, and CuOH, for example.<sup>5–7</sup> But recently we have shown that alkaline earth metal M(OH)<sub>2</sub> molecules can be prepared by the reaction of excited metal atoms with H<sub>2</sub>O<sub>2</sub> or H<sub>2</sub> + O<sub>2</sub> mixtures in condensing argon

and characterized by matrix IR spectroscopy.<sup>8,9</sup> This method can be extended to more exotic metals and used for tetrahydroxides.

An opportunity to form a metal tetrahydroxide is presented by tetravalent hafnium despite the extraordinary stability of the hafnium dioxide product. Atomic Hf is very reactive: ground-state Hf inserts into O<sub>2</sub> to make OHfO, and excited Hf reacts with H<sub>2</sub> to produce HfH<sub>2</sub> and even more HfH<sub>4</sub>.<sup>10,11</sup> Hence a reaction between Hf and H<sub>2</sub>O<sub>2</sub> is possible, but will the tetrahydroxide product be formed and will it be stable?

## Experimental and Theoretical Methods

Experimentally, laser-ablated Hf atoms were reacted with H<sub>2</sub>O<sub>2</sub> molecules in excess argon during condensation onto a 10 K cesium iodide window as described previously.<sup>10–12</sup> Urea-hydrogen peroxide (Aldrich) at room temperature provided H<sub>2</sub>O<sub>2</sub> molecules to the flowing argon reaction medium. Deuterated urea-D<sub>2</sub>O<sub>2</sub> was prepared by adapting methods described previously.<sup>13,14</sup> Infrared spectra were recorded on a Nicolet 750 spectrometer after sample deposition, after annealing, and after irradiation by a common mercury arc street lamp. Complementary experiments were performed with H<sub>2</sub> and O<sub>2</sub> mixtures in order to introduce <sup>18</sup>O<sub>2</sub> into the product molecules.<sup>8,9</sup> Theoretically, the structures and vibrational

\* Author to whom correspondence should be addressed. E-mail: lsa@virginia.edu.

- (1) Cotton, F. A.; Wilkinson, G.; Murillo, C. A.; Bochmann, M. *Advanced Inorganic Chemistry*, 6th ed.; Wiley: New York, 1999.
- (2) (a) Wells, A. F. *Structural Inorganic Chemistry*, 4th ed.; Clarendon Press: Oxford, 1975. (b) McWhan, D. B.; Lundgren, G. *Inorg. Chem.* **1966**, *5*, 284. (c) Hansson, M. *Acta Chem. Scand.* **1969**, *23*, 3541.
- (3) Greenwood, N. N.; Earnshaw, A. *Chemistry for the Elements*, 2nd ed.; Butterworth-Heinemann: Oxford, U.K. 1997.
- (4) Holleman, A. F.; Wiberg, E. *Lehrbuch der Anorganischen Chemie*, 101; Wiberg, N., Ed.; Walter de Gruyter: Berlin, New York, 1995.
- (5) Higgins, K. J.; Friend, S. M.; Klemperer, W.; Apponi, A. J.; Ziurys, L. M. *J. Chem. Phys.* **2004**, *121*, 11715.
- (6) Li, M.; Coxon, J. A. *J. Chem. Phys.* **1995**, *102*, 2663; **1996**, *104*, 4961 and references therein.
- (7) Whitham, C. J.; Ozeki, H.; Saito, S. *J. Chem. Phys.* **2000**, *112*, 641 and references therein.

- (8) Andrews, L.; Wang, X. *Inorg. Chem.* **2005**, *44*, 11.
- (9) Wang, X.; Andrews, L. *J. Phys. Chem. A* **2005**, *109*, 2782.
- (10) Chertihin, G. V.; Andrews, L. *J. Phys. Chem.* **1995**, *99*, 6356.
- (11) Chertihin, G. V.; Andrews, L. *J. Phys. Chem.* **1995**, *99*, 15004.
- (12) Andrews, L. *Chem. Soc. Rev.* **2004**, *33*, 123 and references therein.
- (13) Pettersson, M.; Tuominen, S.; Rasanen, M. *J. Phys. Chem. A* **1997**, *101*, 1166.
- (14) Pehkonen, S.; Pettersson, M.; Lundell, J.; Khriachtchev, L.; Rasanen, M. *J. Phys. Chem. A* **1998**, *102*, 7643.

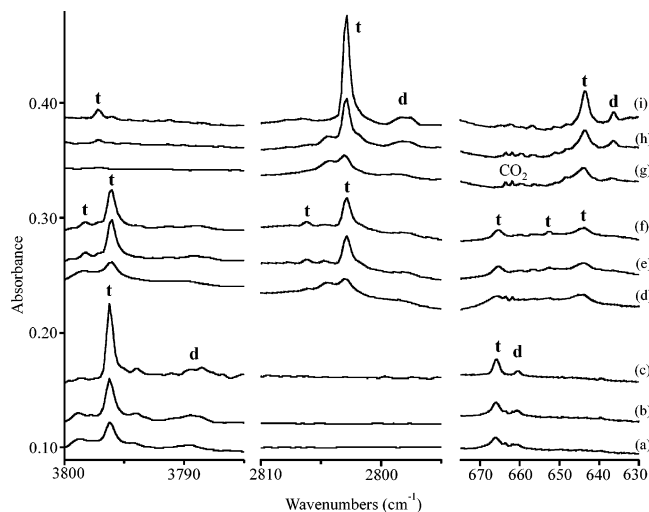


**Figure 1.** Infrared spectra of Hf atom and  $\text{H}_2\text{O}_2$  reaction products in excess argon at 10 K. (a) Hf +  $\text{H}_2\text{O}_2$ , (b) after annealing to 20 K, (c) after annealing to 40 K, (d) Hf +  $\text{H}_2\text{O}_2$  +  $\text{D}_2\text{O}_2$ , (e) after annealing to 26 K, (f) after annealing to 38 K, (g) Hf +  $\text{D}_2\text{O}_2$ , (h) after annealing to 24 K, and (i) after annealing to 32 K.

frequencies of the  $\text{Hf}(\text{OH})_4$  and  $\text{Hf}(\text{OH})_2$  molecules were calculated using the MP2 method and the medium 6-311++G(d,p) basis set for O and H atoms.<sup>15,16</sup> Relativistic effects were included in the SDD pseudopotential for hafnium (12 valence electrons).<sup>17</sup> All bond lengths and bond angles were varied, and the converged minima are stable structures with all real frequencies. Reaction energies are from MP2 results with zero point energy corrections.

## Results and Discussion

Infrared spectra of the major Hf +  $\text{H}_2\text{O}_2$  and Hf +  $\text{D}_2\text{O}_2$  reaction products are compared in Figure 1. New absorptions were observed at 3796.2 and 666.0  $\text{cm}^{-1}$  (labeled **t**) and at 3788.6 and 660.6  $\text{cm}^{-1}$  (labeled **d**), which shifted to 2803.0 and 643.6  $\text{cm}^{-1}$  (**t**) or 2797.9 and 636.5  $\text{cm}^{-1}$  (**d**) with  $\text{D}_2\text{O}_2$ . These bands increased substantially at the expense of  $\text{H}_2\text{O}_2$  on sample annealing to allow diffusion and reaction of trapped species, and the **t** bands increased slightly with ultraviolet ( $\lambda > 220$  nm) irradiation. In contrast, weak matrix site absorptions observed at 3799.0 and 2804.5  $\text{cm}^{-1}$  above the major **t** bands on sample deposition disappeared on annealing into the 32–40 K range (Figure 1c,i). A weak **t** absorption at 3797.2  $\text{cm}^{-1}$  arises from the reaction of the approximately 10%  $\text{HDO}_2$  in the  $\text{D}_2\text{O}_2$  sample (Figure 1i). The **t** absorptions are very sharp with full-widths at half-

maximum of 0.6 and 1.5  $\text{cm}^{-1}$ , respectively. Higher  $\text{H}_2\text{O}_2$  concentration markedly favored the **t** over the **d** bands. The major product absorptions are listed in Tables 1 and 2. In addition, weak absorptions observed for  $\text{HfO}_2$  (902.7, 1626.7  $\text{cm}^{-1}$ ),  $\text{DHfO}$  (901.1, 1165.8  $\text{cm}^{-1}$ ), and  $\text{HfO}_2$  (813.8, 883.3  $\text{cm}^{-1}$ ) remained unchanged while **t** and **d** bands increased on annealing.<sup>10,18</sup>

One experiment was done using simultaneous co-deposition of Ar/ $\text{H}_2\text{O}_2$  and Ar/ $\text{D}_2\text{O}_2$  streams with Hf atoms, and the hydrogen peroxide precursor spectra (not shown) revealed no evidence of isotopic exchange. The major product bands increased on annealing at 3796.2 and 2803.0  $\text{cm}^{-1}$  as before along with one weaker new mixed isotopic component at 3798.3 and at 2806.2  $\text{cm}^{-1}$ , and weak **d** bands appeared at 3788.6 and 2797.9  $\text{cm}^{-1}$ . The lower frequency region revealed **t** bands at 665.6, 653.0, and 643.8  $\text{cm}^{-1}$ , and a very weak **d** band at 657.1  $\text{cm}^{-1}$  (Figure 1d,e,f).

Experiments were performed with Hf and  $\text{H}_2$  or  $\text{D}_2$  +  $\text{O}_2$  as the reagent, and infrared spectra are shown in Figure 2. The **t** bands were observed at 3796.4 and 666.0  $\text{cm}^{-1}$  with 3-fold weaker intensity, but the **d** bands at 3788.8 and 660.6  $\text{cm}^{-1}$  were comparable. However, the  $\text{HfO}_2$  absorptions were much stronger,  $\text{HfH}_2$  was detected at 1622.4  $\text{cm}^{-1}$ , and stronger  $\text{HfH}_4$  bands were observed at 1678.5 and 1675.7  $\text{cm}^{-1}$  as reported previously.<sup>11</sup> The product bands shifted when  $^{16}\text{O}_2$  was replaced by  $^{18}\text{O}_2$ , and additional isotopic splittings were observed with the  $\text{H}_2$  +  $^{16}\text{O}_2$  +  $^{16}\text{O}^{18}\text{O}$  +  $^{18}\text{O}_2$  and with the  $\text{HD}$  +  $\text{O}_2$  reagent mixtures.

The sharp major product **t** absorptions at 3796.4 and 666.0  $\text{cm}^{-1}$ , which are associated by common annealing behavior, are characterized as O–H and Hf–O stretching modes by the effect of isotopic substitution. First, the 3796.4  $\text{cm}^{-1}$  band shifts to 2803.2  $\text{cm}^{-1}$  with deuterium (H/D isotopic frequency ratio 1.3543) and to 3784.4  $\text{cm}^{-1}$  with oxygen-18 (16/18 isotopic frequency ratio 1.00317), which are appropriate for an O–H stretching mode.<sup>8,9</sup> Second, the 666.0  $\text{cm}^{-1}$  band shifts to 639.1  $\text{cm}^{-1}$  with oxygen-18 (16/18 ratio 1.03933), which is lower than that observed for the antisymmetric Hf–O stretching mode in  $\text{HfO}_2$  (ratio 1.05345).<sup>10</sup> The deuterium shift to 643.6  $\text{cm}^{-1}$  shows that H(D) motion is also involved in this normal mode.

Next, the mixed isotopic spectra identify the molecular stoichiometry of the new reaction products. The  $\text{H}_2$  +  $^{16}\text{O}_2$  +  $^{16}\text{O}^{18}\text{O}$  +  $^{18}\text{O}_2$  reagent gave the same major **t** bands as found with  $^{16}\text{O}_2$  and  $^{18}\text{O}_2$  separately plus weak additional bands at 3799.1, 3797.9, 3787.3, 3786.2, and 3785.2  $\text{cm}^{-1}$  in the O–H stretching region and at 684.8, 682.2, 676.7, 651.8, and 645.9  $\text{cm}^{-1}$  in the Hf–O stretching region. Reaction with  $\text{HD}$  and  $^{16}\text{O}_2$  produced analogous spectra with even more obvious new mixed isotopic product absorptions: The major bands shifted slightly to 3796.3 and 2803.2  $\text{cm}^{-1}$  and weak new peaks were observed at 3799.7, 3798.6, 3797.2 (shoulder), 2808.1, 2806.4, and 2804.8  $\text{cm}^{-1}$  in the upper region and major bands at 667.6 and 645.6  $\text{cm}^{-1}$  and weak peaks at 663.6 and 649.4  $\text{cm}^{-1}$  in the lower region (Figure 2d).

- (15) Frisch, M. J.; Trucks, G. W.; Schlegel, H. B.; Scuseria, G. E.; Robb, M. A.; Cheeseman, J. R.; Zakrzewski, V. G.; Montgomery, J. A., Jr.; Stratmann, R. E.; Burant, J. C.; Dapprich, S.; Millam, J. M.; Daniels, A. D.; Kudin, K. N.; Strain, M. C.; Farkas, O.; Tomasi, J.; Barone, V.; Cossi, M.; Cammi, R.; Mennucci, B.; Pomelli, C.; Adamo, C.; Clifford, S.; Ochterski, J.; Petersson, G. A.; Ayala, P. Y.; Cui, Q.; Morokuma, K.; Malick, D. K.; Rabuck, A. D.; Raghavachari, K.; Foresman, J. B.; Cioslowski, J.; Ortiz, J. V.; Stefanov, B. B.; Liu, G.; Liashenko, A.; Piskorz, P.; Komaromi, I.; Gomperts, R.; Martin, R. L.; Fox, D. J.; Keith, T.; Al-Laham, M. A.; Peng, C. Y.; Nanayakkara, A.; Gonzalez, C.; Challacombe, M.; Gill, P. M. W.; Johnson, B. G.; Chen, W.; Wong, M. W.; Andres, J. L.; Head-Gordon, M.; Replogle, E. S.; Pople, J. A. *Gaussian 98*, revision A; Gaussian, Inc.: Pittsburgh, PA, 1998 and references therein.
- (16) Frisch, M. J.; Pople, J. A.; Binkley, J. S. *J. Chem. Phys.* **1984**, *80*, 3265.
- (17) Andrae, D.; Haeussermann, U.; Dolg, M.; Stoll, H.; Preuss, H. *Theor. Chim. Acta* **1990**, *7*, 123.

- (18) Zhou, M. F.; Zhang, L. N.; Dong, J.; Qin, Q. *Z. J. Am. Chem. Soc.* **2000**, *122*, 10680.

**Table 1.** Observed and Calculated Frequencies (cm<sup>-1</sup>) for Hf(OH)<sub>4</sub> in the T<sub>d</sub> Structure

| mode         | Hf(OH) <sub>4</sub> |  | Hf(OH) <sub>2</sub> (OD) <sub>2</sub> |                              | Hf(OD) <sub>4</sub> |                  | Hf( <sup>18</sup> O) <sub>4</sub> |        |
|--------------|---------------------|--|---------------------------------------|------------------------------|---------------------|------------------|-----------------------------------|--------|
|              | obsd <sup>a</sup>   | calcd <sup>b</sup>                         | obsd                                  | calcd                        | obsd                | calcd            | obsd                              | calcd  |
| O–H stretch  |                     | 4070.0 (a <sub>1</sub> , 0) <sup>c,d</sup> | 3798.6<br>3796.4                      | 4067.8 (172)<br>4065.7 (346) |                     | 2969.8 (0)       |                                   | 4055.9 |
| O–H stretch  | 3796.4              | 4065.7 (t <sub>2</sub> , 345 × 3)          | 2806.4<br>2803.2                      | 2966.7 (125)<br>2963.6 (248) | 2803.2              | 2963.6 (248 × 3) | 3784.4                            | 4051.9 |
| Hf–O stretch |                     | 695.9 (a <sub>1</sub> , 0)                 | 691.7<br>663.6                        | 688.1 (17)<br>663.6 (207)    |                     | 674.7 (0)        |                                   | 658.3  |
| Hf–O stretch | 666.0               | 663.3 (t <sub>2</sub> , 197 × 3)           | 653.7<br>645.6                        | 652.3 (181)<br>646.5 (189)   | 643.6               | 646.4 (198 × 3)  | 639.1                             | 632.5  |
| Hf–O–H bend  |                     | 299.7 (t <sub>2</sub> , 510 × 3)           |                                       | 298.7 (293)<br>290.6 (448)   |                     | 247.7 (270 × 3)  |                                   | 295.7  |

<sup>a</sup> Observed t bands from hydrogen plus oxygen reaction products in solid argon. <sup>b</sup> Calculated at MP2/6-311++G(d,p)/SDD level. <sup>c</sup> Mode symmetry in T<sub>d</sub>, infrared intensity, km/mol. <sup>d</sup> Additional frequencies calculated at 297.4 (e, 0 × 2), 266.6 (t<sub>1</sub>, 0 × 3), 183.8 (t<sub>2</sub>, 5 × 3), and 178.7 (e, 0 × 2).

**Table 2.** Observed and Calculated Frequencies (cm<sup>-1</sup>) for Hf(OH)<sub>2</sub> in the C<sub>2v</sub> Structure

| mode         | Hf(OH) <sub>2</sub> |  | Hf(OH)(OD) |              | Hf(OD) <sub>2</sub> |              | Hf( <sup>18</sup> O) <sub>2</sub> |        |
|--------------|---------------------|--|------------|--------------|---------------------|--------------|-----------------------------------|--------|
|              | obsd <sup>a</sup>   | calcd <sup>b</sup>                       | obsd       | calcd        | obsd                | calcd        | obsd                              | calcd  |
| O–H stretch  |                     | 4030.9 (a <sub>1</sub> , 9) <sup>c</sup> | 3789.0     | 4031.1 (242) |                     | 2940.2 (5)   |                                   | 4017.1 |
| O–H stretch  | 3788.8              | 4031.2 (b <sub>2</sub> , 474)            | 2799.4     | 2939.5 (171) | 2797.9              | 2938.7 (337) | 3776.7                            | 4017.6 |
| Hf–O stretch |                     | 702.9 (a <sub>1</sub> , 0)               |            | 694.5 (14)   |                     | 681.7 (0)    |                                   | 664.9  |
| Hf–O stretch | 660.6               | 661.6 (b <sub>2</sub> , 244)             | 649.4      | 651.6 (225)  | 636.5               | 645.4 (232)  | 635.6                             | 632.3  |
| Hf–O–H bend  |                     | 507.7 (b <sub>2</sub> , 13)              | 488.7      | 495.8 (92)   |                     | 380.6 (6)    |                                   | 504.1  |
| Hf–O–H bend  |                     | 494.1 (a <sub>2</sub> , 0)               |            | 487.5 (95)   |                     | 378.2 (96)   |                                   | 490.8  |
| Hf–O–H bend  |                     | 483.2 (a <sub>1</sub> , 184)             |            | 378.6 (55)   |                     | 376.9 (92)   |                                   | 477.7  |
| Hf–O–H bend  | 471.4               | 481.2 (b <sub>1</sub> , 191)             |            | 374.5 (48)   |                     | 370.2 (0)    | 467.1                             | 475.2  |
| O–Hf–O bend  |                     | 51.3 (a <sub>1</sub> , 13)               |            | 49.0 (12)    |                     | 46.7 (11)    |                                   | 49.4   |

<sup>a</sup> Observed d bands in solid argon. <sup>b</sup> Calculated at MP2/6-311++G(d,p)/SDD level. <sup>c</sup> Mode symmetry in C<sub>2v</sub>, infrared intensity, km/mol.

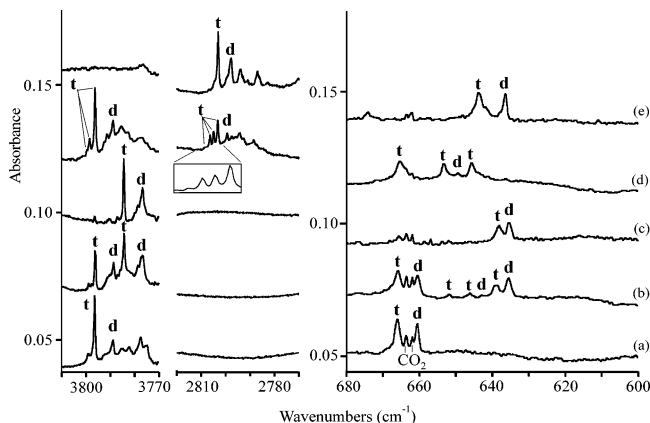
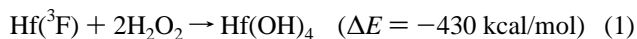


**Figure 2.** Infrared spectra of the Hf atom and H<sub>2</sub> + O<sub>2</sub> reaction products in excess argon at 10 K after full-arc irradiation and annealing to 24–30 K. (a) H<sub>2</sub> + <sup>16</sup>O<sub>2</sub>, (b) H<sub>2</sub> + <sup>16</sup>O<sub>2</sub> + <sup>16</sup>O<sup>18</sup>O + <sup>18</sup>O<sub>2</sub>, (c) H<sub>2</sub> + <sup>18</sup>O<sub>2</sub>, (d) HD + <sup>16</sup>O<sub>2</sub>, and (e) D<sub>2</sub> + <sup>16</sup>O<sub>2</sub>.

The mixed isotopic patterns, particularly the new absorptions observed with HD + O<sub>2</sub>, suggest a product with more than two OH subgroups, and the straightforward reaction product Hf(OH)<sub>4</sub> was computed using the MP2 method with all structural parameters varied. The calculation converged rigorously to T<sub>d</sub> symmetry and gave all real frequencies, which are listed in Table 1. The Hf reaction with two H<sub>2</sub>O<sub>2</sub> molecules is highly exothermic, but can this energy be dissipated and the molecule trapped? In principle Hf(OH)<sub>4</sub> is a very stable molecule. The calculated tetrahedral structure with linear Hf–O–H bonds is depicted in Figure 3:



The agreement between calculated and observed frequencies is striking. The MP2 method is expected to overestimate

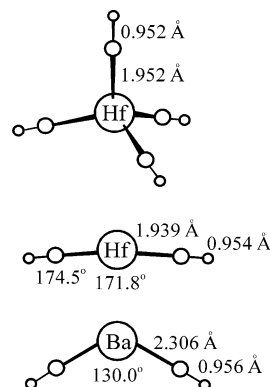


**Figure 3.** Structures calculated for Hf(OH)<sub>4</sub> and Hf(OH)<sub>2</sub> at the MP2/6-311++G(d,p)/SDD level of theory allowing all bond lengths and angles to vary giving converged T<sub>d</sub> and C<sub>2v</sub> structures with all real frequencies. Structure of Ba(OH)<sub>2</sub> taken from ref 9.

observed anharmonic frequencies,<sup>19</sup> and our calculation for H<sub>2</sub>O<sub>2</sub> provides a frequency calibration scale factor observed/calculated = 3588/3848 = 0.932. This scale factor times our MP2 calculated antisymmetric O–H stretching frequency for Hf(OH)<sub>4</sub> predicts 3791 cm<sup>-1</sup>, which is very near the 3796.4 cm<sup>-1</sup> observed value. The MP2 computed antisymmetric Hf–O stretching mode is 663.3 cm<sup>-1</sup>, and we observe this band at 666.0 cm<sup>-1</sup>. Furthermore, the MP2 calculation predicts 16.9 and 30.8 cm<sup>-1</sup> D and <sup>18</sup>O shifts, and we observe 22.4 and 26.9 cm<sup>-1</sup> isotopic shifts. This mostly antisymmetric O–Hf–O stretching mode has slightly more D and less O character than calculated at the MP2 level of theory.

The best evidence for the tetrahydroxide identification of the major product species is to form the new Hf(OH)<sub>2</sub>(OD)<sub>2</sub> isotopic modification in addition to Hf(OH)<sub>4</sub> and Hf(OD)<sub>4</sub>

(19) Scott, A. P.; Radom, L. *J. Phys. Chem.* **1996**, *100*, 16502.

using  $\text{H}_2\text{O}_2 + \text{D}_2\text{O}_2$  as the reagent. The  $\text{Hf}(\text{OH})_2(\text{OD})_2$  molecule has lower symmetry, and all four O–H(D) and Hf–OH(D) stretching modes are allowed. We observe these four bands with the proper shifts relative to  $\text{Hf}(\text{OH})_4$  and  $\text{Hf}(\text{OD})_4$  (see Figure 1d,e,f and Table 1). The symmetric O–H and O–D stretching modes for  $\text{Hf}(\text{OH})_2(\text{OD})_2$  are new bands at  $3798.6$  and  $2806.4 \text{ cm}^{-1}$ , and the antisymmetric O–H and O–D stretching modes for  $\text{Hf}(\text{OH})_2(\text{OD})_2$  coincide with these strong modes for  $\text{Hf}(\text{OH})_4$  and  $\text{Hf}(\text{OD})_4$ . Our calculation for  $\text{Hf}(\text{OH})_2(\text{OD})_2$  predicts  $2.1$  and  $3.1 \text{ cm}^{-1}$  separations between these symmetric and antisymmetric modes, and we observe  $2.2$  and  $3.2 \text{ cm}^{-1}$  separations. The  $\text{HD} + \text{O}_2$  reaction is more complicated, and all five  $\text{Hf}(\text{OH})_{n-4}(\text{OD})_n$  ( $n = 0, 1, 2, 3, 4$ ) product molecules are formed. In addition to  $\text{Hf}(\text{OH})_4$ ,  $\text{Hf}(\text{OH})_2(\text{OD})_2$ , and  $\text{Hf}(\text{OD})_4$  described above, we find new bands for  $\text{Hf}(\text{OH})_3(\text{OD})$  and  $\text{Hf}(\text{OH})(\text{OD})_3$  at  $3799.7$  and  $2804.8 \text{ cm}^{-1}$  and at  $3797.2$  and  $2808.1 \text{ cm}^{-1}$  in the upper region and at  $663.6$  and  $649.4 \text{ cm}^{-1}$  in the lower region, respectively, based on comparison with calculated frequencies (not given here). Thus, the strong  $3796.4 \text{ cm}^{-1}$  band contains contributions from antisymmetric O–H stretching modes of isotopic molecules containing 2, 3, and 4 OH groups, and the strong  $2803.2 \text{ cm}^{-1}$  band likewise arises from antisymmetric O–D stretching modes of molecules with 2, 3, and 4 OD subunits. The same applies to the mixed  $^{16}\text{O}_2 + ^{16}\text{O}^{18}\text{O} + ^{18}\text{O}_2$  precursor where the five  $\text{Hf}(^{16}\text{OH})_{n-4}(^{18}\text{OH})_n$  ( $n = 0, 1, 2, 3, 4$ ) product molecules are observed based on comparison with calculated frequencies. The major  $\text{Hf}(^{16}\text{OH})_2(^{18}\text{OH})_2$  isotopic species exhibits the stronger new peaks at  $3799.1$  and  $3786.2 \text{ cm}^{-1}$  in the upper region and at  $645.9 \text{ cm}^{-1}$  in the lower region. The excellent agreement between observed and calculated frequencies for  $\text{Hf}(\text{OH})_4$ , and particularly the mixed H, D and  $^{16}\text{O}$ ,  $^{18}\text{O}$  isotopic modifications, confirms our identification of  $\text{Hf}(\text{OH})_4$ , which is the first definitive evidence for a metal tetrahydroxide molecule. Furthermore, the observation of sharp bands for two triply degenerate vibrational modes suggests that high symmetry predicted by the MP2 calculation is retained in the matrix cage.

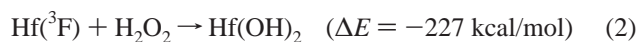
The weaker **d** bands fall in the same regions and are favored with lower  $\text{H}_2\text{O}_2$  concentration and in  $\text{H}_2 + \text{O}_2$  samples. Our MP2 calculations for  $\text{Hf}(\text{OH})_2$  predict  $34.5$  and  $1.7 \text{ cm}^{-1}$  lower O–H and Hf–O stretching frequencies than our calculation for  $\text{Hf}(\text{OH})_4$ , and the **d** bands are  $7.6$  and  $5.4 \text{ cm}^{-1}$  lower (Table 2). The almost linear structure (Figure 3) for  $\text{Hf}(\text{OH})_2$  is between the structures computed for the highly ionic  $\text{Ca}(\text{OH})_2$  and  $\text{Sr}(\text{OH})_2$  molecules.<sup>8,9,20</sup> Of more importance, both O–H and O–D stretching modes, one Hf–O stretching mode, and a Hf–O–H bending mode are observed for  $\text{Hf}(\text{OH})(\text{OD})$ , which are in excellent agreement with calculated values. We also find unshifted O–H stretching modes for  $\text{Hf}(^{16}\text{OH})(^{18}\text{OH})$  and the Hf–O stretching mode at  $643.0 \text{ cm}^{-1}$  as predicted by calculations. Accordingly, the **d** bands are assigned to  $\text{Hf}(\text{OH})_2$ , which is the first report of a Group 4 dihydroxide molecule.

(20) Kaupp, M.; Schleyer, P. v. R. *J. Am. Chem. Soc.* **1992**, *114*, 491.

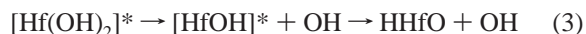
**Table 3.** Mulliken Charges Computed for Metal Hydroxide Molecules

| molecule                 | $q(\text{M})$ | $q(\text{O})$ | $q(\text{H})$ |
|--------------------------|---------------|---------------|---------------|
| $\text{Ba}(\text{OH})_2$ | 1.66          | −1.25         | 0.42          |
| $\text{Hf}(\text{OH})_2$ | 0.58          | −0.75         | 0.46          |
| $\text{Hf}(\text{OH})_4$ | 1.43          | −0.75         | 0.39          |

The  $\text{Hf}(\text{OH})_2$  molecule is also stable ( $^1\text{A}_1$  ground state), and exothermic reaction 2 appears to be spontaneous in the matrix as well as reaction 1, based on the growth of **t** and **d** absorptions on annealing. We do not, however, observe an increase of  $\text{HfO}_2$  on this annealing, which suggests that  $\text{Hf}(\text{OH})_2$  and  $\text{Hf}(\text{OH})_4$  are stable molecules under the conditions of our matrix isolation experiment. Fast relaxation of the energized  $\text{Hf}(\text{OH})_2$  product is required for its stabilization in the matrix. Finally,  $\text{Hf}(\text{OH})_2$  is extremely reactive, and it adds another  $\text{H}_2\text{O}_2$  molecule to give  $\text{Hf}(\text{OH})_4$  with almost the same exothermicity:



The  $\text{HfOH}$  monohydroxide molecule is not observed, but the  $21 \text{ kcal/mol}$  more stable  $\text{H}=\text{Hf}=\text{O}$  isomer is formed on sample deposition with both  $\text{H}_2\text{O}_2$  and  $\text{H}_2 + \text{O}_2$  reagents. We suggest that slow matrix relaxation of the reaction 2 product  $\text{Hf}(\text{OH})_2$  allows the stable  $\text{HHfO}$  fragment to be formed:



The  $\text{H}_2\text{O}_2$  reactions with Zr give similar spectra, which can be assigned to  $\text{Zr}(\text{OH})_4$  and  $\text{Zr}(\text{OH})_2$ , and the analogous reactions are almost as exothermic. The zirconium and hafnium hydroxides are isostructural as expected from parallels in zirconium and hafnium chemistry.<sup>11,21</sup> The metal atom reaction with  $\text{H}_2\text{O}_2$  in excess argon has therefore provided access to a new molecule type, the metal tetrahydroxide.

The structures of  $\text{Hf}(\text{OH})_4$  and  $\text{Hf}(\text{OH})_2$  are of interest, and they are compared with the structure calculated<sup>9,20</sup> for  $\text{Ba}(\text{OH})_2$  in Figure 3. First, notice that the M–O–H bonds are all computed to be linear for the  $T_d$  structure of  $\text{Hf}(\text{OH})_4$  and nearly linear for the  $C_{2v}$  structure of  $\text{Hf}(\text{OH})_2$ , which indicates a high degree of ionic bonding.<sup>7,22</sup> Also notice, however, that the O–H stretching frequencies ( $3796$  and  $3788 \text{ cm}^{-1}$  for the Hf compounds and  $3724 \text{ cm}^{-1}$  for  $\text{Ba}(\text{OH})_2$ ) do not reach the gaseous  $\text{OH}^-$  value ( $3556 \text{ cm}^{-1}$ ).<sup>23</sup> The computed Mulliken charges (Table 3) show more ionic character for  $\text{Ba}(\text{OH})_2$  than for  $\text{Hf}(\text{OH})_2$  as expected from the simple ionization energies ( $120 \text{ kcal/mol}$  for Ba and  $161 \text{ kcal/mol}$  for Hf following the effect of lanthanide contraction).<sup>1,21</sup> However, notice the substantial increase in charge on Hf in the tetrahydroxide as compared to the dihydroxide, which is needed to support four negatively charged OH units in the stable  $\text{Hf}(\text{OH})_4$  molecule.

(21) Pyykko, P. *Chem. Rev.* **1988**, *88*, 563.

(22) Ikeda, S.; Nakajima, T.; Hirao, K. *Mol. Phys.* **2003**, *101*, 105.

(23) Rosenbaum, N. H.; Owruksy, J. C.; Tack, L. M.; Saykally, R. J. *J. Chem. Phys.* **1986**, *84*, 5308.



### Structure of the $\text{Hf}(\text{OH})_4$ Molecule

So why then has solid  $\text{Hf}(\text{OH})_4$  not been prepared if the molecule is so stable? The dehydration of  $\text{Hf}(\text{OH})_4$  gives  $\text{HfO}_2$ , which is a very stable refractory solid, like zirconia,<sup>1</sup> and the coordinative saturation and oligomerization of  $\text{HfO}_2$  will probably foster decomposition of  $\text{Hf}(\text{OH})_4$  in the solid phase. The standard heats of formation of  $\text{HfO}_2$  (solid) ( $-274$  kcal/mol) and of Hf (gas) atoms ( $148$  kcal/mol)<sup>24</sup> and our computed energy for  $\text{HfO}_2(\text{g})$  give the heat of condensation of  $\text{HfO}_2$  as  $-240$  kcal/mol. It thus appears that  $\text{Hf}(\text{OH})_4$  will be unstable in the solid phase. This postulate has credence in the fact that solid  $\text{Zr}(\text{OH})_2\text{SO}_4$  complexes contain  $(\text{ZrO}_2)_n$  chains of the type found in the solid zirconia structure.<sup>2</sup>

### Conclusions

In summary, the major product in the reaction of laser-ablated Hf atoms with  $\text{H}_2\text{O}_2$  and with  $\text{H}_2$  and  $\text{O}_2$  mixtures

(24) *CRC Handbook, Chemical Thermodynamic Properties*, D-89, 66th ed.; CRC Press: Boca Raton, FL, 1985.

gives rise to two sharp absorptions at  $3796.4$  and  $660.0\text{ cm}^{-1}$ . MP2 calculations with no angles fixed converge rigorously to a tetrahedral  $\text{Hf}(\text{OH})_4$  structure with all real frequencies, which include strong antisymmetric O–H and Hf–O stretching modes in excellent agreement with the observed absorptions. New bands in the reaction with  $\text{H}_2\text{O}_2$  and  $\text{D}_2\text{O}_2$  mixtures can be assigned to  $\text{Hf}(\text{OH})_2(\text{OD})_2$ , and additional new bands observed with  $\text{HD} + \text{O}_2$  are also due to  $\text{Hf}(\text{OH})_3(\text{OD})$  and  $\text{Hf}(\text{OH})(\text{OD})_3$  based on comparison with calculated isotopic frequencies. Thus, the stable  $\text{Hf}(\text{OH})_4$  molecule is identified from matrix infrared spectra through mixed isotopic substitution and calculation of isotopic frequencies.

**Acknowledgment.** We gratefully acknowledge financial support from NSF Grant CHE03-53487 and helpful e-mail correspondence with L. Khriachtchev, S. Pehkonen, and P. Pyykko.

IC050614A